Int J Theor Phys (2009) 48: 803–814
DOI 10.1007/s10773-008-9854-3

Wigner Functions and Tomograms of the Even and Odd Negative Binomial States

Xiao-Yan Zhang · Ji-Suo Wang · Xiang-Guo Meng · Jie Su

Received: 7 July 2008 / Accepted: 11 September 2008 / Published online: 24 September 2008

Abstract Using the coherent state representation of Wigner operator and the technique of integration within an ordered product (IWOP) of operators, the Wigner functions of the even and odd negative binomial states (NBSs) are obtained. We concentrate our analysis on the fact that the even and odd NBSs interpolate between the even and odd coherent states and the even and odd quasi-thermal states depending on the values of the parameters involved. Moreover, the tomograms of the even and odd NBSs are calculated by virtue of intermediate coordinate-momentum representation in quantum optics.

Keywords Quantum optics · Even and odd negative binomial state · IWOP technique · Wigner function · Tomogram · Nonclassical effect

1 Introduction

In the field of quantum optics, much attention has been paid to superpositions of quantum states (so-called quantum state engineering) because they exhibit nonclassical properties such as sub-Poissonian distributions, antibunching, and quadrature squeezing [9, 12]. These states are closely related to some probability distribution functions, such as the binomial state [13] links to the binomial distribution, while the negative binomial state (NBS) corresponds to the negative binomial distribution, etc. Recently, Fan [6] introduced the even and odd negative binomial states, since the even and odd NBSs are "intermediate" between even and odd coherent states and even and odd thermal (pure) states, by varying their parameters one can move systematically from coherent states character to thermal states character. As far as we know, not enough attention has been paid to the fact that the even and odd NBSs actually interpolate between the "most classical" pure state allowed in quantum theory (the coherent state) and the "less classical" one (the thermal state). In our opinion, the interesting

Project 10574060 supported by the National Natural Science Foundation of China and project Q2007A01 supported by the Natural Science Foundation of Shandong Province.

X.-Y. Zhang · J.-S. Wang (✉) · X.-G. Meng · J. Su
School of Physical Science and Information Engineering, Liaocheng University, Shandong Province, 252059, People's Republic of China
e-mail: jswang@lcu.edu.cn

feature places the even and odd NBSs in a unique situation, justifying by themselves a more careful examination of their interpolation properties. This is the main purpose of this paper.

Therefore, we would like to present a detailed study of the nonclassical properties for the even and odd NBSs, including squeezing properties, sub-Poissonian character, behavior of the quasiprobability distributions. The Wigner function [1, 3, 17] in phase space plays an important role in modern quantum optics. Experimentally, various photon states have been generated by the micromaser [2, 14] and the Wigner functions of some cavity fields can be measured in the whole phase space by a scheme based on interaction between cavity fields and atoms [18, 19]. Recently, it was found that using the optical tomography was possible to measure the quantum state. A generalization of the optical tomography method leads to introducing the tomogram, which can be considered as a new representation of quantum mechanics and the new representation of quantum states has been used analyze the probability [11]. Therefore, it is significance to construct and measure the Wigner functions and the tomograms of quantum states by using some theoretical schemes.

This paper is organized as follows. In Sect. 2, we present a short review of the even and odd NBSs, and discussing some of their nonclassical features. In Sect. 3, we investigate their nonclassical (or interpolation) properties in phase space (Wigner functions and tomograms of the even and odd NBSs). Finally, the main conclusions are given in Sect. 4.

2 Statistical Properties of the Even and Odd NBSs

The NBS is constructed by a linear combination of numbers states with coefficients chosen in such a way that the photon number distribution is NBS

$$|\eta,s,\varphi\rangle=\sum_{n=0}^{\infty}\sqrt{b(n,\eta,s)}e^{in\varphi}|n\rangle,\quad b(n,\eta,s)\equiv\binom{n+s}{n}\eta^{s+1}(1-\eta)^n, \tag{1}$$

where s $(s\geq 0)$ is any real positive number, $0<\eta<1$, $n=0,1,2,\ldots$. The mean of photon number distribution corresponding to the state (1) is given by

$$\overline{n}=(1+s)(1-\eta)/\eta. \tag{2}$$

In [5], the even and odd NBSs are defined as, respectively,

$$|\eta,s,\varphi\rangle_e=N_e\sum_{n=0}^{\infty}\sqrt{\binom{2n+s}{2n}\eta^{s+1}(1-\eta)^{2n}e^{i2n\varphi}}|2n\rangle, \tag{3a}$$

$$|\eta,s,\varphi\rangle_o=N_o\sum_{n=0}^{\infty}\sqrt{\binom{2n+1+s}{2n+1}\eta^{s+1}(1-\eta)^{2n+1}e^{i(2n+1)\varphi}}|2n+1\rangle, \tag{3b}$$

where the normalization constants N_e and N_o are obtained from the normalization condition ${}_{e,o}\langle\eta,s,\varphi|\eta,s,\varphi\rangle_{e,o}=1$, so that

$$N_e=\sqrt{\frac{2}{1+(2/\eta-1)^{-s-1}}},\qquad N_o=\sqrt{\frac{2}{1-(2/\eta-1)^{-s-1}}}, \tag{4}$$

here the subscripts "e" or "o" mean even or odd. Respectively, the states $|\eta,s,\varphi\rangle_e$ and $|\eta,s,\varphi\rangle_o$ reduce to even and odd coherent states in the limiting condition of parameters:

$s \to \infty, \eta \to 0$, such that $(1+s)(1-\eta)/\eta \equiv \overline{n}$ is kept constant. While in another limiting condition $s \to 0, 0 < \eta < 1$, the states $|\eta, s, \varphi\rangle_e$ and $|\eta, s, \varphi\rangle_o$ reduce to so-called even and odd thermal (pure) states.

Now, we study quadrature squeezing for the even and odd NBSs, the quadrature operators X_1 and X_2 are defined as

$$X_1 = (a + a^\dagger)/2, \qquad X_2 = (a - a^\dagger)/(2i). \tag{5}$$

The quadrature operators X_1 and X_2 do not commute, i.e., $[X_1, X_2] = i/2 \neq 0$, and they obey the uncertainty relation

$$\left\langle \Delta X_1^2 \right\rangle \left\langle \Delta X_2^2 \right\rangle \geq 1/16. \tag{6}$$

In order to examine the squeezing degree of the light field, we define the squeezing degree in the following form:

$$D_1 = 2\left\langle a^\dagger a \right\rangle + \left\langle a^{\dagger 2} + a^2 \right\rangle - \left\langle a^\dagger + a \right\rangle^2, \tag{7}$$

$$D_2 = 2\left\langle a^\dagger a \right\rangle - \left\langle a^{\dagger 2} + a^2 \right\rangle + \left\langle a^\dagger + a \right\rangle^2. \tag{8}$$

If D_j $(j = 1, 2)$ satisfies the conditions $-1 \leq D_j < 0$, the light field shows quadrature squeezing effect in the X_j $(j = 1, 2)$ direction, and the maximum squeezing (100%) is obtained when $D_j = -1$.

For the even and odd NBSs, the squeezing exists in the X_2 quadrature, thus we produced a plot of D_2 as a function of η for different values of $\overline{n}$, which can be appreciated in Fig. 1

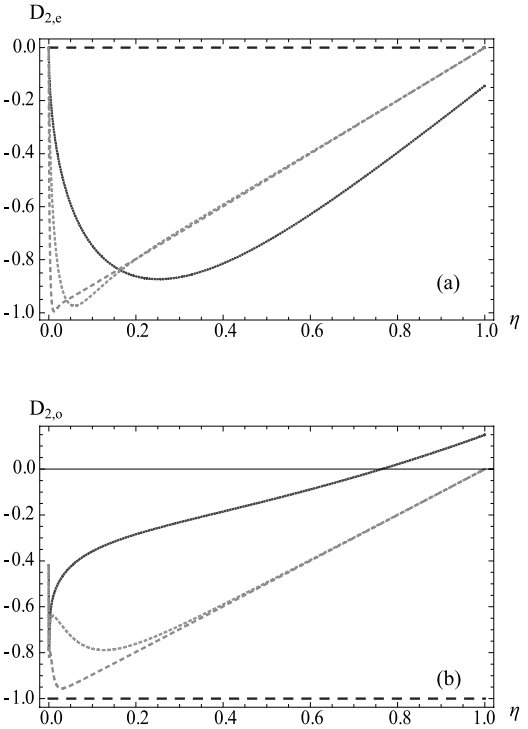

Fig. 1 Quadrature squeezing of the even NBS (**a**) and odd NBS (**b**) with η, $\bar{n} = 2$ (*solid curve*), $\bar{n} = 10$ (*dotted curve*) and $\bar{n} = 50$ (*broken curve*)

(in order to simplify the calculation we set $\varphi = 0$). We note that the even and odd NBSs exhibit squeezing, and the squeezing degree is sensitive to the value of the mean of photon number $\overline{n}$. With $\overline{n}$ increasing, the depth of the squeezing increases. However, for the lower value of $\overline{n}$, when η is larger the odd NBS does not exhibit squeezing, the even NBS always exists squeezing with different $\overline{n}$ in the range of η.

Let us consider the second-order correlation function $g^{(2)}(0)$ for the even and odd NBSs given by (3a) and (3b). The function $g^{(2)}(0)$ is defined as

$$g^{(2)}(0) = \left\langle a^{\dagger 2} a^2 \right\rangle / \left\langle a^{\dagger} a \right\rangle^2 . \tag{9}$$

If $g^{(2)}(0) < 1$, it means that a state exhibits sub-Poissonian distribution (i.e., antibunching effect).

The second-order correlation function $g^{(2)}_{e,o}(0)$ for the even and odd NBSs are given by, respectively

$$g^{(2)}_e(0) = \frac{\sum_{n=0}^{\infty} \frac{(2n+s)!}{(2n-2)!s!} \eta^{s+1} (1-\eta)^{2n}}{|N_e|^2 [\sum_{n=0}^{\infty} \frac{(2n+s)!}{(2n-1)!s!} \eta^{s+1} (1-\eta)^{2n}]^2}, \tag{10}$$

$$g^{(2)}_o(0) = \frac{\sum_{n=0}^{\infty} \frac{(2n+1+s)!}{(2n-1)!s!} \eta^{s+1} (1-\eta)^{2n+1}}{|N_o|^2 [\sum_{n=0}^{\infty} \frac{(2n+1+s)!}{(2n)!s!} \eta^{s+1} (1-\eta)^{2n+1}]^2}. \tag{11}$$

From (10) and (11) we can plot $g^{(2)}_{e,o}(0)$ against η when $\overline{n} = 2$, 10, 50 in Fig. 2. We can see clearly that when $g^{(2)}_o(0) < 1$, the odd NBS exhibits sub-Poissonian distribution for

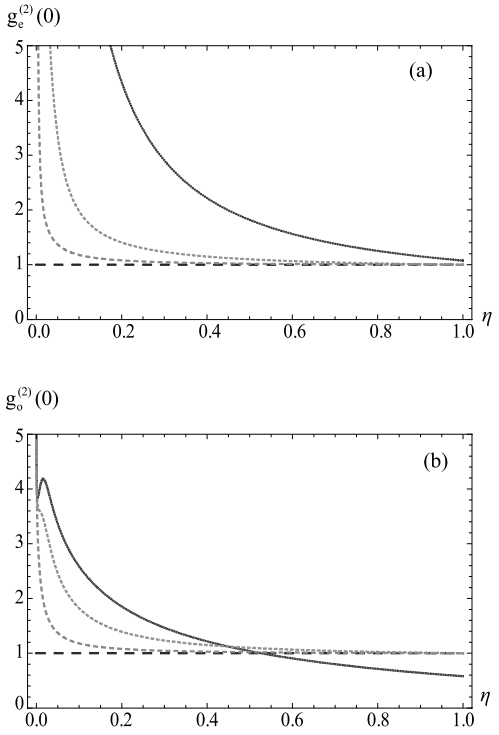

Fig. 2 Sub-Poissonian behaviour of the even NBS (**a**) and odd NBS (**b**) with η, $\bar{n} = 2$ (*solid curve*), $\bar{n} = 10$ (*dotted curve*) and $\bar{n} = 50$ (*broken curve*)

the lower value of $\overline{n}$. However, the even NBS always exhibits super-Poissonian behavior (bunching effect) for the complete range of η. With $\overline{n}$ increasing, the values of $g_e^{(2)}(0)$ and $g_o^{(2)}(0)$ begin to reduce, the values remain around 1 for the even and odd NBSs. In a word, the nonclassical nature of the odd NBS is apparent when the mean of photon number is very small.

3 Wigner Functions of the Even and Odd NBSs

Wigner function is an effective tool in quantum optics, which can give a good indication about the possibility of occurrence of nonclassical effects. Furthermore, it is well-behaved function and sensitive to interference in phase space. With the study of the Wigner functions of the even and odd NBSs, one can characterize the non-classical nature of the states. In the coherent state representation, the Wigner operator $\Delta(\alpha,\alpha^*)$ is [7]

$$\Delta\left(\alpha,\alpha^*\right)=\int\frac{d^2z}{\pi}\left|\alpha+z\right\rangle\left\langle\alpha-z\right|e^{\alpha z^*-\alpha^* z}, \tag{12}$$

where $|\alpha+z\rangle$ is the coherent state [8, 10] and α is a complex number. By virtue of the technique of integration within an ordered product (IWOP) of operators [4, 7], the Wigner operator $\Delta(\alpha,\alpha^*)$ is simplified as

$$\Delta\left(\alpha,\alpha^*\right)=\frac{2}{\pi}D\left(2\alpha\right)\left(-\right)^N, \tag{13}$$

where $N=a^+a$, $D(2\alpha)=\exp[2(\alpha a^+-\alpha^* a)]$ is the displaced operator.

For a pure state $|\psi\rangle$, we can express as

$$\left|\psi\right\rangle=\sum_{n=0}^{\infty}f_n\left|n\right\rangle, \tag{14}$$

its Wigner function is

$$W\left(\alpha,\alpha^*\right)=\left\langle\psi\right|\Delta\left(\alpha,\alpha^*\right)\left|\psi\right\rangle=\frac{2}{\pi}\sum_{m,n=0}^{\infty}f_m^*f_n\left(-1\right)^m\chi_{mn}\left(2\alpha\right), \tag{15}$$

where

$$\chi_{mn}\left(2\alpha\right)=\begin{cases}\sqrt{\frac{n!}{m!}}(2\alpha)^{m-n}\exp(-2|\alpha|^2)L_n^{m-n}(4|\alpha|^2), & m\geq n,\\ \sqrt{\frac{m!}{n!}}(-2\alpha^*)^{n-m}\exp(-2|\alpha|^2)L_m^{n-m}(4|\alpha|^2), & m<n,\end{cases} \tag{16}$$

where $L_n^m(x)$ denotes an associated Laguerre polynomials [16]

$$L_n^m\left(x\right)=\sum_{l=0}^{n}\binom{n+m}{n-l}\frac{(-x)^l}{l!}. \tag{17}$$

By mathematical calculation, the Wigner functions $W_e(\alpha,\alpha^*)$ of the states $|\eta,s,\varphi\rangle_e$ given by (3a) can be expressed as a sum of the mixture part $W_e^M(\alpha,\alpha^*)$ and quantum interference part $W_e^I(\alpha,\alpha^*)$ [15]

$$W_e\left(\alpha,\alpha^*\right)=W_e^M\left(\alpha,\alpha^*\right)+W_e^I\left(\alpha,\alpha^*\right), \tag{18}$$

where the mixture part $W_e^M(\alpha,\alpha^*)$ is found to be

$$W_e^M(\alpha,\alpha^*) = \frac{4}{\pi[1+(2/\eta-1)^{-s-1}]}\exp(-2|\alpha|^2) \times \sum_{n=0}^{\infty}(-1)^{2m}\binom{2n+s}{2n}\eta^{s+1}(1-\eta)^{2n}L_{2n}(4|\alpha|^2), \tag{19a}$$

and the quantum interference part $W_e^I(\alpha,\alpha^*)$ has the following form

$$\begin{aligned} W_e^I(\alpha,\alpha^*) = {} & \frac{4}{\pi[1+(2/\eta-1)^{-s-1}]}\exp(-2|\alpha|^2)\sum_{\substack{m,n=0\\ m\neq n}}^{\infty}(-1)^{2m}\eta^{s+1} \\ & \times\sqrt{\binom{2n+s}{2n}\binom{2m+s}{2m}(1-\eta)^{2(m+n)}} \\ & \times e^{2i(n-m)\varphi}\left[\sqrt{\frac{(2n)!}{(2m)!}}(2\alpha)^{2(m-n)}L_{2n}^{2(m-n)}(4|\alpha|^2)\right. \\ & \left.+\sqrt{\frac{(2m)!}{(2n)!}}\left(-2\alpha^*\right)^{2(n-m)}L_{2m}^{2(n-m)}(4|\alpha|^2)\right]. \end{aligned} \tag{19b}$$

Similarly, using (3b), (15), and (16) we also obtain the Wigner functions $W_o(\alpha,\alpha^*)$ of the states $|\eta,s,\varphi\rangle_o$. The mixture part $W_o^M(\alpha,\alpha^*)$ and the quantum interference part $W_o^I(\alpha,\alpha^*)$ are given by, respectively

$$W_o^M(\alpha,\alpha^*) = \frac{4}{\pi[1-(2/\eta-1)^{-s-1}]}\exp(-2|\alpha|^2)\sum_{n=0}^{\infty}(-1)^{2m+1} \times\binom{2n+1+s}{2n+1}\eta^{s+1}(1-\eta)^{2n+1}L_{2n+1}(4|\alpha|^2), \tag{20}$$

$$\begin{aligned} W_o^I(\alpha,\alpha^*) = {} & \frac{4}{\pi[1-(2/\eta-1)^{-s-1}]}\exp(-2|\alpha|^2)\sum_{\substack{m,n=0\\ m\neq n}}^{\infty}(-1)^{2m+1}\eta^{s+1} \\ & \times\sqrt{\binom{2n+1+s}{2n+1}\binom{2m+1+s}{2m+1}(1-\eta)^{2(m+n+1)}} \\ & \times e^{2i(n-m)\varphi}\left[\sqrt{\frac{(2n+1)!}{(2m+1)!}}(2\alpha)^{2(m-n)}L_{2n+1}^{2(m-n)}(4|\alpha|^2)\right. \\ & \left.+\sqrt{\frac{(2m+1)!}{(2n+1)!}}\left(-2\alpha^*\right)^{2(n-m)}L_{2m+1}^{2(n-m)}(4|\alpha|^2)\right]. \end{aligned} \tag{21}$$

By means of numerical computation (in order to simplify the calculation we set $\varphi=0$), the Wigner functions of the even and odd NBSs are plotted for different values of parameters η and s against $\alpha=\mathrm{Re}\,\alpha+\mathrm{Im}\,\alpha$, and keep the mean number of photons $\overline{n}=3$ constant in

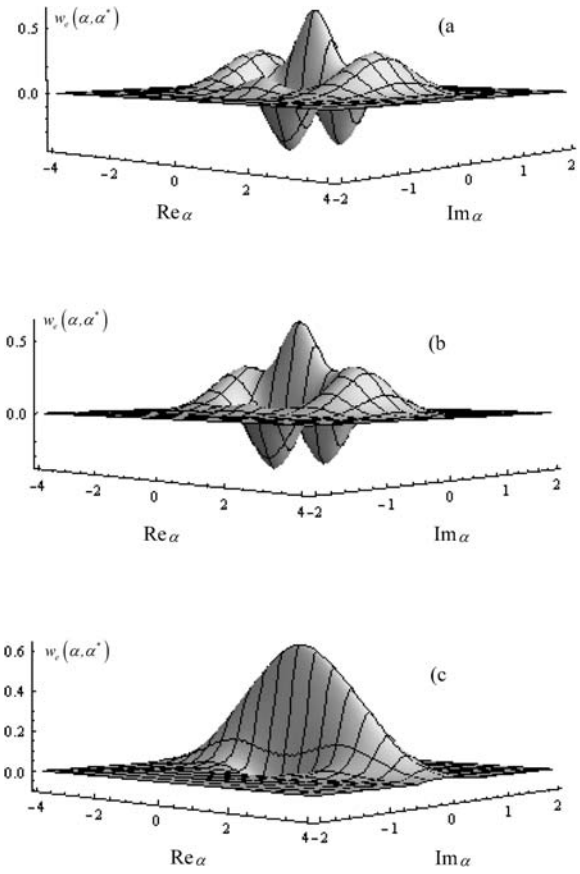

Fig. 3 Wigner function of the even NBS with Re α and Im α, $\bar{n} = 3$ is kept constant. (**a**) $\eta = 0.97$, $s = 96$ (coherent state limit); (**b**) $\eta = 0.7$, $s = 6$; and (**c**) $\eta = 0.25$, $s = 0$ (thermal state limit)

Figs. 3 and 4, respectively. We would like to discuss the variation of the Wigner functions with different parameters η and s ($\eta = 0.97$, $s = 96$, $\eta = 0.7$, $s = 6$, and $\eta = 0.25$, $s = 0$) in phase space. We find that the Wigner distributions of the even and odd NBSs are real functions which can take negative values in limited regions of phase space. Therefore, the nonclassical effects can be established. When $\eta = 0.97$, $s = 96$ in Fig. 3(a), the Wigner function of the even NBS $W_e(\alpha, \alpha^*)$ displays one prominent upward peak and two downward peaks at the origin of phase space. However, there are two upward peaks and only one prominent downward peak in Fig. 4(a) which plot the odd NBS $W_o(\alpha, \alpha^*)$ with the same parameters at the same position in the phase space. Thus, the feature indicates that the even NBS and odd NBS are orthogonal. With the decreasing η (or increasing s), for the same mean number of photons $\overline{n} = 3$, we can see clearly that the downward peak values begin to reduce in Fig. 3 and the nonclassical effect becomes weaker obviously. On the contrary, in Fig. 4, with decreasing η (or increasing s) for the same mean number of photons $\overline{n} = 3$, the downward peak values increase, and the nonclassical effect becomes stronger. Compared the case of the even and odd coherent states limit (Figs. 3(a) and 4(a)) with the thermal limit (Figs. 3(c) and 4(c)), we note that the oscillatory part is very different from each other in two cases. The width of the Gaussian peak is associated with the variance of the coherent field. If we move to a typical even (odd) NBS with $\overline{n} = 3$ (when $\eta = 0.7$, $s = 6$), the Wigner function will still show the two Gaussian-like peaks (Figs. 3(b) and 4(b)) and the some os-

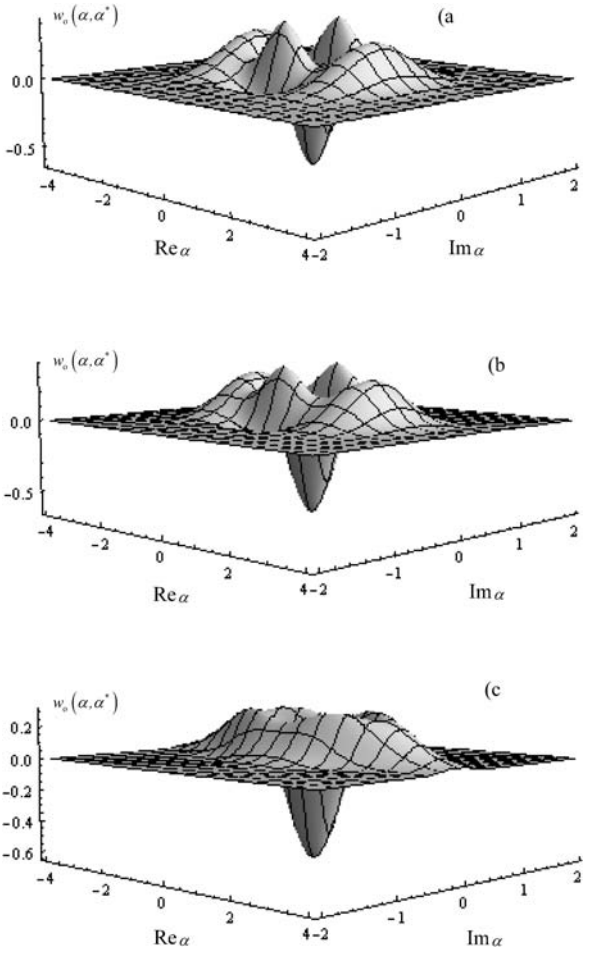

Fig. 4 Wigner function of the odd NBS with Re α and Im α, $\bar{n} = 3$ is kept constant. (**a**) $\eta = 0.97$, $s = 96$ (coherent state limit); (**b**) $\eta = 0.7$, $s = 6$; and (**c**) $\eta = 0.25$, $s = 0$ (thermal state limit)

cillations between these peaks. However, the widths of the so-called Gaussian-like peaks are much broader than the coherent state case. Thus, the quasi-probability distributions for the even and odd NBSs are different from the even and odd coherent states.

Finally, we move to the other extreme of the even and odd NBSs known as the even and odd thermal states by setting parameters $\eta = 0.25$, $s = 0$, and $\overline{n} = 3$. The Wigner functions for the even and odd quasi-thermal states are depicted in Figs. 3(c) and 4(c), respectively. In this case, the changes of the Wigner functions are very interesting. We can see the Gaussian-like peaks broadened largely and only one prominent peak (positive in the even state and negative in the odd state) along with a few oscillations. We find a reduced nonclassical character in the even quasi-thermal state and a reduced interference in both even and odd thermal state. Another interesting aspect is the quadrature squeezing. In phase space, squeezing manifests itself as an actual deformation of the quasiprobabilites. Also with η decreasing, we can see the squeezing from the figures and the squeezing becomes stronger. Just as a matter of speculation, we could draw a parallel between the negative growth of the Wigner function and the linear increase of sub-Poissonian character of the even NBS. Therefore, we can find that the Wigner function $W_{e,o}(\alpha, \alpha^*)$ have different squeezing, sub-Poissonian distributions and quasiprobability distributions for different parameters η, s and the same mean number

of photons $\overline{n} = 3$ from Figs. 3 and 4, namely the even and odd NBSs exhibit remarkably different quantum effects. In conclusion, the behavior of the Wigner functions $W_{e,o}(\alpha, \alpha^*)$ is in agreement with the quantum features of the states.

4 Tomograms of the Even and Odd NBSs

In recent year, the use of tomograms in quantum mechanics and quantum optics provides the possibility of describing a quantum state with a positive probability distribution. A direct description of quantum states by means of quantum tomograms for the system observably is interesting from both the theoretical and experimental points of view. Therefore, tomogram approach has brought much interest of some physicists. In this section we derive the tomograms of the states $|\eta, s, \varphi\rangle_{e,o}$ which are defined as

$$T_{e,o}(q, f, g) = \iint_{\infty} dp' dx' \delta(q - fq' - gp') W_{e,o}(q', p'), \tag{22}$$

where $W_{e,o}(q', p')$ is the Wigner functions for the states $|\eta, s, \varphi\rangle_{e,o}$. However, it will be very difficult to evaluate the integration if we directly substitute (19a), (19b) into (22), luckily, we can use the following Radon transform between the Wigner operator and the projection operator $|q\rangle_{f,g\,f,g}\langle q|$ of intermediate coordinate-momentum state [5]

$$|q\rangle_{f,g\,f,g}\langle q| = \iint_{\infty} dp' dx' \delta(q - fq' - gp') \Delta(q', p'). \tag{23}$$

Thus, the tomograms of the states $|\eta, s, \varphi\rangle_{e,o}$ given by (3a) and (3b) are

$$\begin{aligned} T_{e,o}(q, f, g) &= \iint_{\infty} dp' dx' \delta(q - fq' - gp')_{e,o} \langle \eta, s, \varphi| \Delta(q', p') |\eta, s, \varphi\rangle_{e,o} \\ &= \left|{}_{f,g}\langle q \,|\eta, s, \varphi\rangle_{e,o}\right|^2, \end{aligned} \tag{24}$$

which shows that for tomogram approach there exists intermediate coordinate-momentum state $|q\rangle_{f,g}$, and the Radon transform of the Wigner operator is just the pure-state matrices $|q\rangle_{f,g\,f,g}\langle q|$. As a result, the tomogram of quantum states can be considered as the module-square of the states' wave function in intermediate coordinate-momentum representation. Using the completeness relation of coherent states, we can obtain the tomogram amplitude of the states $|\eta, s, \varphi\rangle_e$

$$\begin{aligned} {}_{f,g}\langle q \,|\eta, s, \varphi\rangle_e &= {}_{f,g}\langle q| \int \frac{d^2\alpha}{\pi} |\alpha\rangle \langle \alpha \,|\eta, s, \varphi\rangle_e \\ &= \left[\pi\left(f^2 + g^2\right)\right]^{-1/4} \sqrt{\frac{2}{1 + (2/\eta - 1)^{-s-1}}} \\ &\quad \times \sum_{n=0}^{\infty} \sqrt{\binom{2n+s}{2n} \eta^{s+1} (1-\eta)^{2n}} e^{i2n\varphi} \sqrt{\frac{1}{(2n)!}} \left[\sqrt{\frac{f - ig}{2(f + ig)}}\right]^{2n} \\ &\quad \times H_{2n}\left(\frac{q}{\sqrt{f^2 + g^2}}\right) \exp\left[-\frac{q^2}{2(f^2 + g^2)}\right], \end{aligned} \tag{25}$$

where the state $|q\rangle_{f,g}$ is expressed as

$$|q\rangle_{f,g}=\frac{1}{[\pi(f^2+g^2)]^{1/4}}\exp\left[-\frac{q^2}{2(f^2+g^2)}+\sqrt{2}a^{\dagger}\frac{q}{f-ig}-\frac{f+ig}{2(f-ig)}a^{\dagger 2}\right]|0\rangle, \tag{26}$$

which is the eigenvector of the operator $(fQ+gP)$ corresponding to the eigenvalue q, f and g are two real parameters. And we also have used the following integral formula

$$\begin{aligned}&\int\frac{d^2z}{\pi}\exp\left[\zeta|z|^2+\xi z+\eta z^*+fz^2+gz^{*2}\right]\\&\quad=\frac{1}{\sqrt{\zeta^2-4fg}}\exp\left[\frac{-\zeta\xi\eta+\xi^2g+\eta^2f}{\zeta^2-4fg}\right],\\&\mathrm{Re}\,(\zeta\pm f\pm g)<0,\qquad \mathrm{Re}\left(\frac{\zeta^2-4fg}{\zeta\pm f\pm g}\right)<0\end{aligned} \tag{27}$$

and the generating function of $H_n(q)$ is

$$H_n(q)=\frac{d^n}{dq^n}\exp\left(2qt-q^2\right)\big|_{t=0}. \tag{28}$$

So we can obtain the tomograms of the states $|\eta,s,\varphi\rangle_e$

$$\begin{aligned}T_e(q,f,g)=&\left[\pi\left(f^2+g^2\right)\right]^{-1/2}\frac{2}{1+(2/\eta-1)^{-s-1}}\exp\left[-\frac{q^2}{(f^2+g^2)}\right]\\&\times\left|\sum_{n=0}^{\infty}\sqrt{\binom{2n+s}{2n}\eta^{s+1}(1-\eta)^{2n}}e^{i2n\varphi}\sqrt{\frac{1}{(2n)!}}\right.\\&\left.\times\left[\sqrt{\frac{f-ig}{2(f+ig)}}\right]^{2n}H_{2n}\left(\frac{q}{\sqrt{f^2+g^2}}\right)\right|^2.\end{aligned} \tag{29}$$

In the same way, we can derive the tomogram functions of the states $|\eta,s,\varphi\rangle_o$

$$\begin{aligned}T_o(q,f,g)=&\left[\pi\left(f^2+g^2\right)\right]^{-1/2}\frac{2}{1-(2/\eta-1)^{-s-1}}\exp\left[-\frac{q^2}{(f^2+g^2)}\right]\\&\times\left|\sum_{n=0}^{\infty}\sqrt{\binom{2n+1+s}{2n+1}\eta^{s+1}(1-\eta)^{2n+1}}e^{i(2n+1)\varphi}\sqrt{\frac{1}{(2n+1)!}}\right.\\&\left.\times\left[\sqrt{\frac{f-ig}{2(f+ig)}}\right]^{2n+1}H_{2n+1}\left(\frac{q}{\sqrt{f^2+g^2}}\right)\right|^2.\end{aligned} \tag{30}$$

In Figs. 5 and 6, we plot the tomograms $T_{e,o}(q,f=\cos\theta,g=\sin\theta)$ of the even and odd NBSs versus (q,θ) for indicated values of the parameters η and s. Tomograms are real and positive distribution functions. As one can see, the tomograms being a function of α, are similar to the Q-functions of the corresponding states. From Fig. 5, with the variation of the coordinate, the tomograms of the even and odd NBSs present π-periodic variations. And,

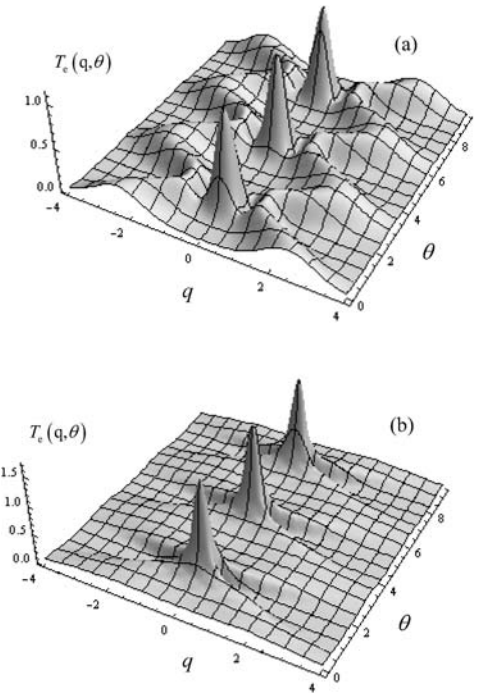

Fig. 5 Tomographic map of the even NBS with q and θ, $\bar{n} = 3$ is kept constant. (**a**) $\eta = 0.97$, $s = 96$ (coherent state limit); (**b**) $\eta = 0.25$, $s = 0$ (thermal state limit)

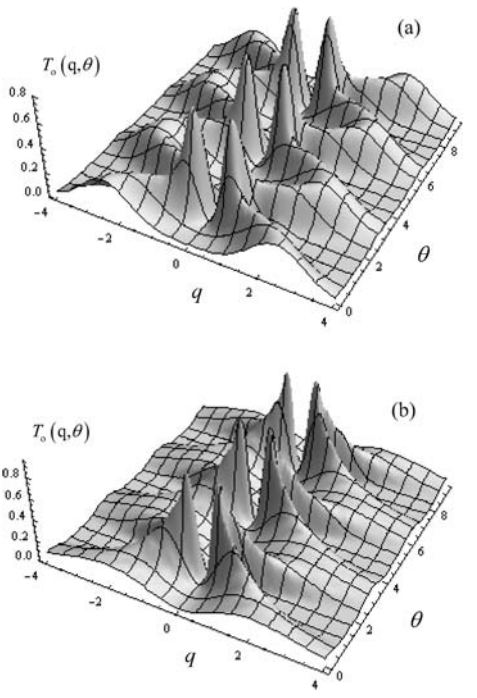

Fig. 6 Tomographic map of the odd NBS with q and θ, $\bar{n} = 3$ is kept constant. (**a**) $\eta = 0.97$, $s = 96$ (coherent state limit); (**b**) $\eta = 0.25$, $s = 0$ (thermal state limit)

we can also clearly see one prominent peak in every period. Furthermore, we can see that at the extreme of the even thermal state ($\eta = 0.25,\ s = 0$), the tomographic distributions become narrower and higher than the even coherent state ($k = 0.96,\ s = 97$) in the phase space. With the increasing η, the interference effects begin to strong. Furthermore, the odd NBS has similar feature as regard to π-periodic variations and interference effects. However, there are two-peak structure in the odd NBS at the origin of phase space. Thus, we can find that the even and the odd NBSs can exhibit different quantum interference effects.

5 Conclusions

In this paper, we have shown that different nonclassical properties are sensitive in a different way to variations in $\overline{n}$, such as quadrature squeezing and sub-Poissonian statistics. we have used the coherent state representation of Wigner operator and the intermediate coordinate-momentum representation to discuss the Wigner functions and the tomograms of the even and odd NBSs. It is found that with the parameters η and s (the tomogram with the parameters q and θ) the variations of the Wigner function distribution of the even and odd NBSs reveal well interference properties. The feature indicates that the even NBS and the odd NBS are orthogonal, and the odd NBS has stronger nonclassical effects in comparison with the even NBS. The results of the tomograms for the even and odd NBSs obtained by using the projection operator of the intermediate coordinate-momentum state $|q\rangle_{f,g\,f,g}\langle q|$ may be useful for experiments as references. Therefore, one can measure the module-square of the wave functions $|\eta, s, \varphi\rangle_{e,o}$ in coherent state representation experimentally, then the tomograms of the even and odd NBSs are obtained and also the states $|\eta, s, \varphi\rangle_{e,o}$ are measured. We also established a link between the quasiprobability distributions and the nonclassical effects. The quasiprobability distributions are valuable tool for understanding subtle aspects of nonclassical behavior in light fields.

Acknowledgements This work was supported by the National Natural Science Foundation of China (No. 10574060) and the Natural Science Foundation of Shandong Province (No. Q2007A01). We acknowledge Prof. H.Y. Fan from University of Science and Technology of China.

References

1. Agarwal, G.S., Wolf, E.: Phys. Rev. D **2**, 2161 (1972)
2. Brattke, S., Vracoe, B.T.H., Walther, H.: Phys. Rev. Lett. **86**, 3534 (2001)
3. Dariano, G., Macchiavello, M.C., Paris, M.G.A.: Phys. Rev. A **50**, 4298 (1994)
4. Fan, H.Y.: Phys. Lett. A **124**, 303 (1987)
5. Fan, H.Y.: Entangled State Representations in Quantum Mechanics and Their Application. Shanghai Jiao Tong Univ. Press, Shanghai (2001)
6. Fan, H.Y., Li, Su.: Commun. Theor. Phys. **43**, 519 (2005)
7. Fan, H.Y., Ruan, T.N.: Commun. Theor. Phys. **3**, 345 (1984)
8. Glauber, R.J.: Phys. Rev. **130**, 2529 (1963)
9. Hillery, M.: Phys. Rev. A **36**, 3796 (1987)
10. Klauder, J.R.: J. Math. Phys. **4**, 1005 (1963)
11. Meng, X.G., Wang, J.S., Fan, H.Y.: Phys. Lett. A **363**, 12 (2007)
12. Monroe, C., et al.: Science **272**, 1131 (1996)
13. Stoler, D., et al.: Opt. Acta **32**, 345 (1985)
14. Vracoe, B.T., Brattke, H.S., Weidinger, M., Walther, H.: Nature **403**, 743 (2000)
15. Wang, J.S., Meng, X.G.: Chin. Phys. B. **17**, 1254 (2008)
16. Wang, Z.X., Guo, D.R.: General Theory of Special Functions. Science Press, Beijing (1965), p. 361 (in Chinese)
17. Wigner, E.P.: Phys. Rev. **40**, 749 (1932)
18. Yang, Q.Y., Wei, L.F., Ding, L.E.: Acta Phys. Sin. **52**, 1390 (2003) (in Chinese)
19. Zhang, Z.M.: Chin. Phys. Lett. **21**, 5 (2004)